AADE-04-DF-HO-45

Non-Isothermal Two-Phase Flow in Naturally Fractured Rock Formations

R.Nair, Halliburton; and Y.Abousleiman, PoroMechanics Institute

This paper was prepared for presentation at the AADE 2004 Drilling Fluids Conference, held at the Radisson Astrodome in Houston, Texas, April 6-7, 2004. This conference was sponsored by the Houston Chapter of the American Association of Drilling Engineers. The information presented in this paper does not reflect any position, claim or endorsement made or implied by the American Association of Drilling Engineers, their officers or members. Questions concerning the content of this paper should be directed to the individuals listed as author/s of this work.

Abstract

An existing finite element model has been extended to incorporate non-isothermal two-phase flow in naturally fractured rock formations. The model accounts for thermo-hydro-mechanical coupling as well as solubility of gas in oil and evaporation of oil into gas in both the rock matrix and fractures. Heat transport by conduction as well as convection has been incorporated into the finite element model in which the displacements, pressures (in the oil and gas phases), and temperature are the primary unknowns. The saturations and capillary pressures are the secondary unknowns evaluated from capillary-saturation-temperature relations. A parametric study is carried out applying the model to the problem of a deviated wellbore drilled under non-isothermal conditions in a fractured rock formation saturated with oil and gas.

Introduction

An increasing number of oil field developments require that challenges posed by high-temperature, high-pressure (HPHT) drilling environments be addressed. Low drilling margins, mud ballooning, or apparent mud loss during circulation, and gas influx are some of the problems faced in such environments.[1,2] Prior to the design of any mud program an accurate estimation of near-wellbore stresses is essential. This requires incorporating fully coupled oil and gas flow under non-isothermal conditions into the analysis. This is because, the compressibilities of oil and gas differ by orders of magnitude. Assuming the formation to be saturated with a single nearly incompressible fluid would lead to an overestimation of near-wellbore stresses and pore pressure and, subsequent planning of mud programs with unnecessarily high mudweights. The presence of natural fractures acting as natural conduits for oil and gas flow in such formations presents an additional level of complexity. Further, fractures affect the compressibility of the rock system and thereby the stresses and pore pressure changes associated with drilling. The significant costs associated with drilling HPHT wells thus warrant an accurate estimation of the stress and pore pressure fields in the vicinity of the wellbore. This may be achieved only by taking into account fully-coupled multiphase flow along with matrix-fracture interactions under non-isothermal conditions.

In this paper, existing mathematical formulations are extended to formulate fully coupled non-isothermal oil-gas flow in a fractured porous media. Specifically, the black oil model has been extended to the limited compositional model to account for thermal effects. The volatility of the oil has been incorporated into the formulation. Thus, the gas phase is comprised of a gas and oil component; the oil phase is comprises of an oil component and a dissolved gas component. In addition, the viscosities of the oil and gas phases, formation volume factors for oil and gas, gas-oil solubility ratio, oil volatility ratio and the saturations are assumed to be dependent on the temperature. The fluid and solid domains are represented by two distinct overlapping continua within the framework of the dual-porosity concept. A single thermodynamic continuum is assumed to be representative of the fractured porous medium. The finite element method is employed to solve the nonlinear set of differential equations, wherein the displacements, pressures (in the oil and gas phases), and temperature are the primary unknowns. The saturations and capillary pressures are the secondary unknowns to be obtained from capillary-saturation-temperature relations. The nonlinear system of equations in the finite element model is solved using a direct solver with iterations employed within each time-step to check the stability. The model is then applied to the problem of an inclined wellbore in a fractured porous medium saturated with oil and gas and a temperature gradient between the drilling and formation fluids. A parametric analysis is carried out to identify influential parameters governing the spatial and temporal distributions of pore pressure, stresses, and temperature in the vicinity of the wellbore.

Mathematical Formulation

The governing equations for non-isothermal two-phase flow in a fractured rock formation will be described. A detailed description of the dual-porosity model illustrating the separate and overlapping approach

has been provided.[3-6] The mass conservation equations for the solid and, oil and gas components are:

$$\frac{\partial\left(1-f^{(h)}\right)r_s^{(h)}}{\partial t}+\frac{\partial\left(1-f^{(h)}\right)r_s^{(h)}u_i^{(h)s}}{\partial x_i}=0 \quad \text{.....(1)}$$

$$\frac{\partial\left(f^{(h)}S_\Pi^{(h)}r_\Pi^{(h)}w_{\Pi\Pi}^{(h)}\right)}{\partial t}+\frac{\partial\left(f^{(h)}S_\Pi^{(h)}r_\Pi^{(h)}U_i^{(h)\Pi}w_{\Pi\Pi}^{(h)}\right)}{\partial x_i}$$
$$+\frac{\partial\left(f^{(h)}S_{\overline{\Pi}}^{(h)}r_{\overline{\Pi}}^{(h)}w_{\Pi\overline{\Pi}}^{(h)}\right)}{\partial t}+\frac{\partial\left(f^{(h)}S_{\overline{\Pi}}^{(h)}r_{\overline{\Pi}}^{(h)}U_i^{(h)\overline{\Pi}}w_{\Pi\overline{\Pi}}^{(h)}\right)}{\partial x_i} \quad \text{..(2)}$$
$$-\Gamma_\Pi=0$$

The Darcy velocities for both fluid phases are:

$$v_i^{(h)\Pi}=f^{(h)}S_\Pi^{(h)}\left(U_i^{(h)\Pi}-u_i^{(h)s}\right) \quad \text{.....(3)}$$

In view of the limited compositional model, the mass fractions of the two components in the two phases are:

$$w_{Og}^{(h)}=\frac{r_{os}^{(h)}R_v^{(h)}}{r_g^{(h)}B_g^{(h)}};\ w_{Oo}^{(h)}=\frac{r_{os}^{(h)}}{r_o^{(h)}B_o^{(h)}}$$
$$w_{Go}^{(h)}=\frac{r_{gs}^{(h)}R_s^{(h)}}{r_o^{(h)}B_o^{(h)}};\ w_{Go}^{(h)}=\frac{r_{gs}^{(h)}}{r_g^{(h)}B_g^{(h)}} \quad \text{.....(4)}$$

The equilibrium (momentum conservation) equation for a dual-porosity medium saturated with oil and gas under non-isothermal conditions may be written as:

$$D_{ijkl}^{I,II}e_{kl}-D_{ijkl}^{I,II}C_{klmn}^{I}a^{I}\left(S_g^I P_g^I+S_o^I P_o^I\right)d_{mn}-$$
$$D_{ijkl}^{I,II}e_{kl}-D_{ijkl}^{I,II}C_{klmn}^{II}a^{II}\left(S_g^{II}P_g^{II}+S_o^{II}P_o^{II}\right)d_{mn}-\text{.....(5)}$$
$$\left(D_{ijkl}^{I,II}\frac{b}{3}Td_{kl}\right)_{,j}+F_i=0$$

Also, the energy balance equation may be written as:

$$\begin{bmatrix}\left(f^I S_g^I r_g^I+f^{II}S_g^{II}r_g^{II}\right)C_{vg}+\\ \left(f^I S_o^I r_o^I+f^{II}S_o^{II}r_o^{II}\right)C_{vo}+\\ \left(1-f^I-f^{II}\right)r_s C_{vs}\end{bmatrix}\frac{\partial T}{\partial t}+$$
$$\begin{bmatrix}\left(r_g^I v_g^I+r_g^{II}v_g^{II}\right)C_{vg}+\\ \left(r_o^I v_o^I+r_o^{II}v_o^{II}\right)C_{vo}+\\ \left(1-f^I-f^{II}\right)r_s C_{vs}\end{bmatrix}.\nabla T- \quad \text{.....(6)}$$
$$\nabla\begin{bmatrix}\left(f^I S_g^I+f^{II}S_g^{II}\right)l_g+\\ \left(f^I S_o^I+f^{II}S_o^{II}\right)l_g+\\ \left(1-f^I-f^{II}\right)l_s\end{bmatrix}.\nabla T+$$
$$\left(1-f^I-f^{II}\right)3KbT\frac{\partial e_{kk}}{\partial t}=0$$

The finite element spatial discretization of equations 1-6 was carried out using the Galerkin's method with the nodal displacements, oil and gas pressures and temperatures as the primary unknowns. The final finite element governing equations are:

Solid Equilibrium:

$$\mathrm{K}\frac{du}{dt}+\mathrm{O}_c^{\mathrm{I}}\frac{dP_o^{\mathrm{I}}}{dt}+\mathrm{O}_c^{\mathrm{II}}\frac{dP_o^{\mathrm{II}}}{dt}+\mathrm{G}_c^{\mathrm{I}}\frac{dP_g^{\mathrm{I}}}{dt}+$$
$$\mathrm{G}_c^{\mathrm{II}}\frac{dP_g^{\mathrm{II}}}{dt}+\mathrm{L}_t\frac{dT}{dt}-\frac{df}{dt}=0 \quad \text{.....(7)}$$

Oil Component:

$$\overline{\mathrm{K}}_o^{(h)}\frac{du}{dt}+\left(\mathrm{O}_D^{(h)}+\mathrm{O}_{tr}\right)\mathrm{P}_o^{(h)}+\left(\mathrm{O}_{eD}^{(h)}+\mathrm{O}_{etr}\right)\mathrm{P}_g^{(h)}-$$
$$\mathrm{O}_{tr}\mathrm{P}_o^{(\overline{h})}-\mathrm{O}_{etr}\mathrm{P}_g^{(\overline{h})}+\mathrm{O}_o^{(h)}\frac{dP_o^{(h)}}{dt}+\mathrm{O}_g^{(h)}\frac{dP_g^{(h)}}{dt} \quad \text{...(8)}$$
$$+\mathrm{S}_{ot}^{(h)}\frac{dT}{dt}=-\overline{\mathrm{Q}}_o^{(h)}$$

Gas Component:

$$\mathrm{K}_g^{(h)}\frac{du}{dt}+\left(\mathrm{G}_{dD}^{(h)}+\mathrm{G}_{dtr}\right)\mathrm{P}_o^{(h)}+\left(\mathrm{G}_D^{(h)}+\mathrm{G}_{tr}\right)\mathrm{P}_g^{(h)}-$$
$$\mathrm{G}_{dtr}\mathrm{P}_o^{(\overline{h})}-\mathrm{G}_{tr}\mathrm{P}_g^{(\overline{h})}+\mathrm{G}_o^{(h)}\frac{dP_o^{(h)}}{dt}+ \quad \text{...(9)}$$
$$\mathrm{G}_g^{(h)}\frac{dP_g^{(h)}}{dt}+\mathrm{S}_{gt}^{(h)}\frac{dT}{dt}=-\overline{\mathrm{Q}}_g^{(h)}$$

Energy Balance:

$$\overline{T}_s \frac{dT}{dt} + \left(\overline{C}_t + \overline{H}_{tF}\right)T + K_t \frac{du}{dt} = -Q_t \quad \text{.....(10)}$$

The temporal discretization is carried out using a finite difference scheme and the values of u, $P_o^{(\eta)}$, $P_g^{(\eta)}$ and T at different times are obtained using a direct solver with convergence checking within each time-step.[3,6]

Application to Inclined Wellbore Geometry

A parametric study of an inclined wellbore is carried out in order to study the effect of phase saturations and dual-porosity parameters for the following cases: (a) single-porosity, two-phase and (b) dual-porosity, two-phase.

Single-Porosity, Two-Phase Modeling

Figs. 1 and 2 show the spatial variations of the oil pressure and effective radial stress for different initial oil saturations. The input parameters are listed in Table 1. The relations between (a) relative permeability and saturation, (b) capillary pressure and saturation, (c) formation volume factors and pressure, temperature, and (d) oil, gas viscosities and temperature, pressure are based on data from literature.[7-9]

The peak in the oil pressure curve (Fig. 1) in the vicinity of the borehole decreases for a lower value of initial oil saturation (S_{oi} = 0.5). Correspondingly, the effective radial and tangential stresses (shown in Figs. 2 and 3) become more compressive for a lower value of initial oil saturation. Due to the low porosity, low heat capacity of gas and lower thermal conductivities of the oil and gas compared to the solid constituent, the initial oil saturation does not affect the temperature distribution as seen in Fig. 4. This may also be attributed to the fact that the thermal diffusivity of the porous medium as a whole (~1.6 x 10^{-6} m^2/s) is higher than the fluid diffusivity (~1.7 x 10^{-7} m^2/s). Hence in this case, heat transport by convection is negligible.

Dual-Porosity, Two-Phase Modeling

The following fracture characteristics were associated with the secondary medium: stiffness (K_n) and fracture spacing (s) (governing the compliance of the secondary medium); secondary porosity (ϕ^{II}) (representing the storativity of the fractures); and, secondary permeability (k^{II}). The formation was assumed to be a dual-porosity medium saturated with oil and gas. The material properties of the primary medium are as in Table 1 whereas the secondary medium parameters are listed in Table 2.

A smaller fracture spacing, increases the overall compliance of the dual-porosity medium thereby resulting in a higher initial oil pressure in the primary medium. This may be observed in Fig. 5, wherein the peak of the oil pressure curve in the primary medium (in the vicinity of the borehole) is highest for a fracture spacing of 0.1 m. This results in tensile effective radial stresses around the borehole, the magnitude of which reduces with an increase in fracture spacing as seen in figure 6. Also, the tangential stresses for a smaller fracture spacing are less compressive (as seen in Fig. 7). The temperature distribution on the other hand, is likely to be unaffected by the secondary medium parameters. The porosity of the secondary medium affects the rate of change in temperature and heat transport by conduction whereas, the fluid diffusivity of the secondary medium affects heat transport by convection. Due to the low fluid diffusivity and storage capacity of the secondary medium (see Table 2), the secondary medium parameters do not affect the temperature distribution (as seen in Fig. 8).

Conclusions

A dual-porosity model incorporating fully coupled non-isothermal flow of oil and gas has been developed based on the "separate" and "overlapping" technique. The model accounts for the solubility of gas in the oil as well as evaporation of oil into the gas phase. The results show that the pore pressure and effective stress distributions in the vicinity of the borehole at short times are affected by the initial oil saturation. In the case of fractured formations, the compliance of the secondary medium governed by the fracture density affects the pore pressure and effective stress distributions. For a medium with low fluid diffusivities, the initial oil saturation and secondary medium parameters do not affect the temperature distributions.

Acknowledgments

This work is supported by the Rock Mechanics Research Center at The University of Oklahoma and the Oklahoma Center for Advancement in Science and Technology and industrial consortium

Nomenclature

Subscripts and Superscripts:

(h) = I,II : I – Primary medium (matrix); II – Secondary medium (fractures)
π = o,g : Oil, gas phase
Π = O, G : Oil, gas component
o, g : Oil, gas phase
s : Solid
I,j,k,l,m,n : Indices as per Einstein's convention

Vectors and Tensors:

$C^{(h)}_{ijkl}$: Compliance tensors
$D^{I,II}_{ijkl}$: Elasticity tensor
F_j : Body forces
U^p_i : Intrinsic velocity of phase p
u^s_i : Solid velocities
v^s_i : Darcy velocities
d_{ij} : Kronecker delta
e_{ij} : Total body strain

Material Parameters:

B_p : *Formation volume factors for phase p*
C_{vp} : *Specific heat of phase p*
R_s : *Gas-solubility ratio*
R_v : *Oil-volatility ratio*
a : *Equivalent Biot's effective stress parameter*
l_p : *Coefficient of thermal conductivity of phase p*
r_p : *Density of phase p under reservoir conditions*
r_{ps} : *Density of phase p under standard conditions*
m_p : *Viscosity of phase p*
f : *Porosity*

Variables:

P_p : *Pressure of phase p*
P_c : *Capillary pressure*
S_p : *Saturation of phase p*
T : *Temperature*
t : *time*
$w_{\tilde{O}p}$: *Mass fraction of component Õ in phase p*
x_i : *Cartesian coordinates*

References

1. Karstad, E. and Aadnoy, B.S.: "Optimization of Mud Temperature and Fluid Models in Offshore Applications," SPE 56939, presented at the 1999 Offshore European Conf., Aberdeen, September 7-9.
2. Bradley, N.D., Low, E., Aas, B., Rommetviet, R. and Larsen, H.F.: "Gas diffusion – Its impact on a horizontal HPHT well," SPE 77474, presented at the 2002 SPE Annual Tech. Conf. Exh., San Antonio, September 29 – October 2.
3. Nair, R.: "The Poromechanics of Naturally Fractured Rock Formations: A Finite Element Approach," *Ph.D. Diss.*, The University of Oklahoma, 2003.
4. Nair, R., Abousleiman, Y. and Zaman, M.: "A Finite Element Porothermoelastic Model for Dual-Porosity Media," To appear in *Int J. Num Anal. Meth. Geomech.,* 2004.
5. Nair, R., Abousleiman, Y. and Zaman, M.: "An Application of the Dual-Porosity Porothermoelastic Approach in Naturally Fractured Porous Media," *In Poromechanics II, Proc. 2nd Biot Conf. on Poromechanics*, Grenoble, pp. 509-514, August 26-28, 2002.
6. Nair, R., Bai, M., Abousleiman, Y. and Zaman, M.: "Finite Element Modeling of an Inclined Wellbore in a Fractured Porous Medium Saturated with Oil and Gas," *Pacific Rocks 2000, Proc. Fourth NAARMS*, Seattle, pp. 189-196, July 31-August 3, 2000.
7. Lewis, R.W. and Ghafouri, H.R.: "A Novel Finite Element Double Porosity Model for Multiphase Flow Through Deformable Porous Media," *Int. J. Num. Anal. Meth. Geomech.*, Vol 21, pp. 789-816, 1997.
8. Ziegler, V.M.: "A Comparison of Steamflood Strategies: Five-spot Pattern vs. Inverted Nine-Spot Pattern," SPE 13620, *SPE Res. Engg.*, pp. 549-558, 1987.
9. Pao, W.K.S., Lewis, R.W. and Masters, I.: "A Fully-Coupled Hydro-Tthermo-Poromechanical Model for Black Oil Reservoir Simulation," *Int. J. Num. Anal. Meth. Geomech.*, Vol. 25, pp. 1229-1256, 2001.

Table 1-Parameters for Single-Porosity, Two-Phase Model

Parameter	Units	Value
Elastic Modulus (E)	MPa	3.55
Poisson's Ratio (ν)	-	0.2
Porosity (ϕ)	-	0.1
Permeability (k)	m^2	10^{-18}
Grain bulk modulus (K_s)	GPa	100
Thermal Expansion Coefficient (β)	$/^0C$	$1.8x10^{-5}$
Solid heat capacity (C_{vs})	$J/kg/^0C$	582
Oil heat capacity (C_{vo})	$J/kg/^0C$	2093
Gas heat capacity (C_{vg})	$J/kg/^0C$	1000
Thermal conductivity of solid (λ_s)	$W/m/^0C$	2.65
Thermal conductivity of oil (λ_o)	$W/m/^0C$	1.3
Thermal conductivity of gas (λ_g)	$W/m/^0C$	0.3
Mudweight	MPa	12
Temperature of drilling fluid	^0C	50

Table 2-Parameters for Dual-Porosity Model

Parameter	Units	Value
Fracture Permeability (k^{II})	m^2	10^{-17}
Fracture stiffness (K_n)	GPa/m	20
Fracture spacing (s)	M	0.1, 0.25, 0.5
Fracture porosity (ϕ^{II})	-	0.02

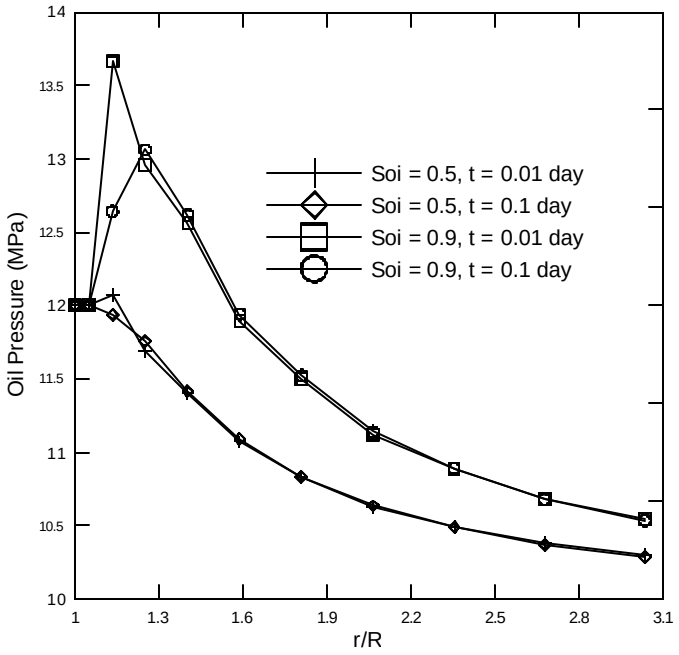

Fig. 1-Oil pressure distribution for different initial oil saturations (single-porosity, two-phase; S_{oi} – initial oil saturations).

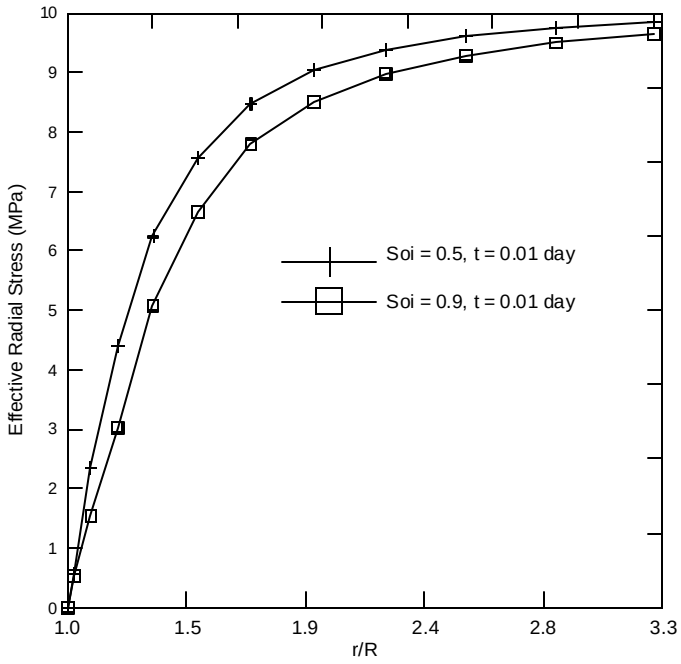

Fig. 2-Effective radial stress distribution for different initial oil saturations (single-porosity, two-phase; S_{oi} – initial oil saturations).

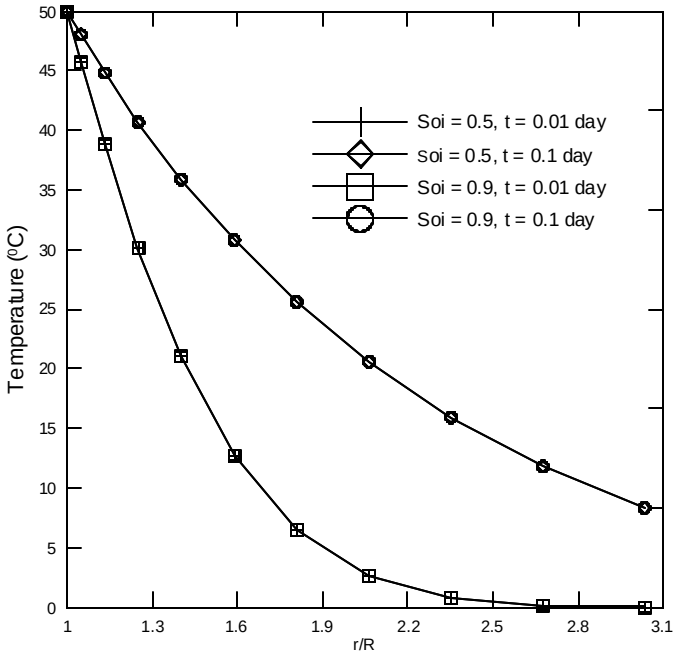

Fig. 4-Temperature distribution for different initial oil saturations (single-porosity, two-phase; S_{oi} – initial oil saturations).

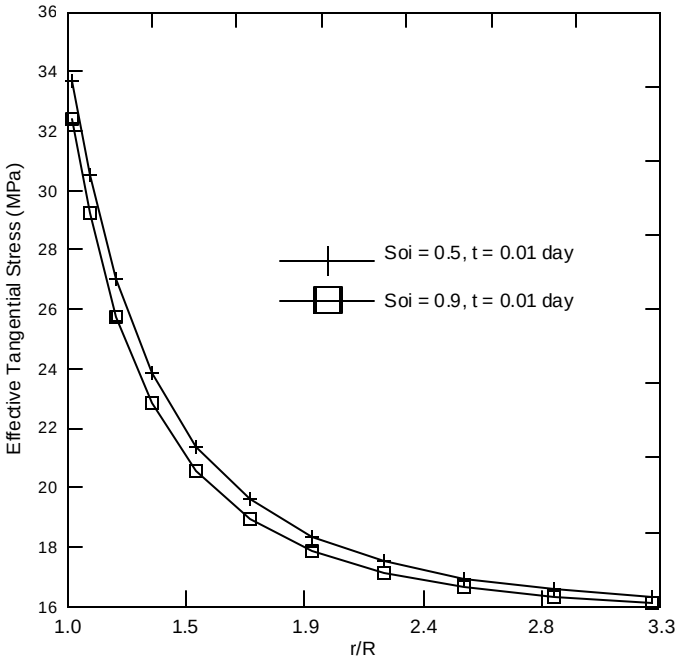

Fig. 3-Effective tangential stress distribution for different initial oil saturations (single-porosity, two-phase; S_{oi} – initial oil saturations).

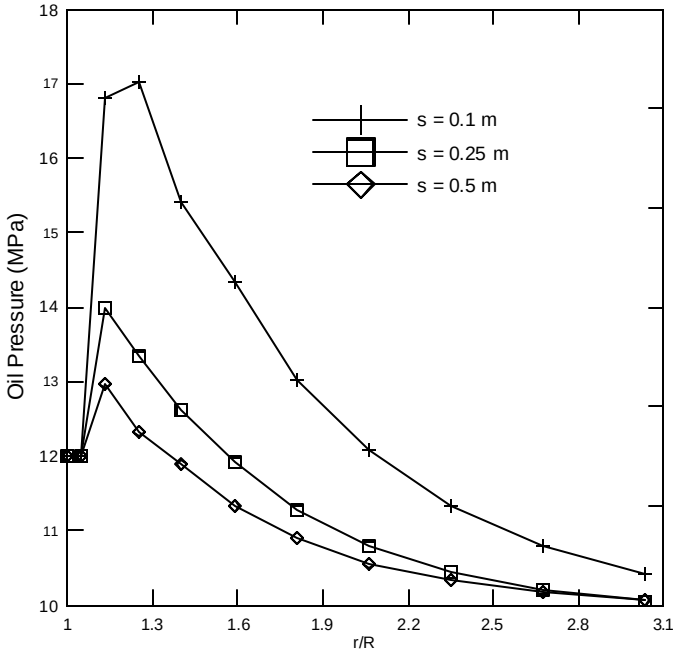

Fig. 5-Primary medium (Matrix) oil pressure distribution for different fracture spacings and initial oil saturation S_{oi} = 0.5 (dual-porosity, two-phase; s – fracture spacing).

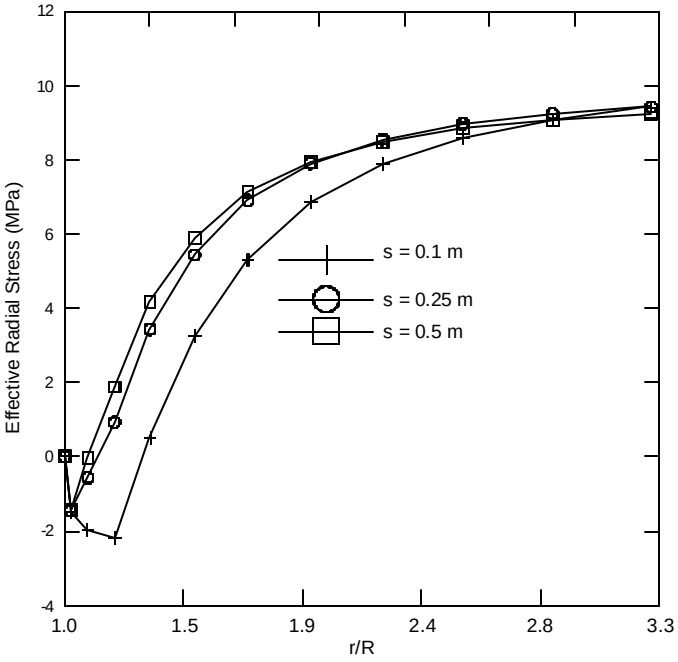

Fig. 6-Effective radial stress distribution for different fracture spacings and initial oil saturation S_{oi} = 0.5 (dual-porosity, two-phase; s – fracture spacing).

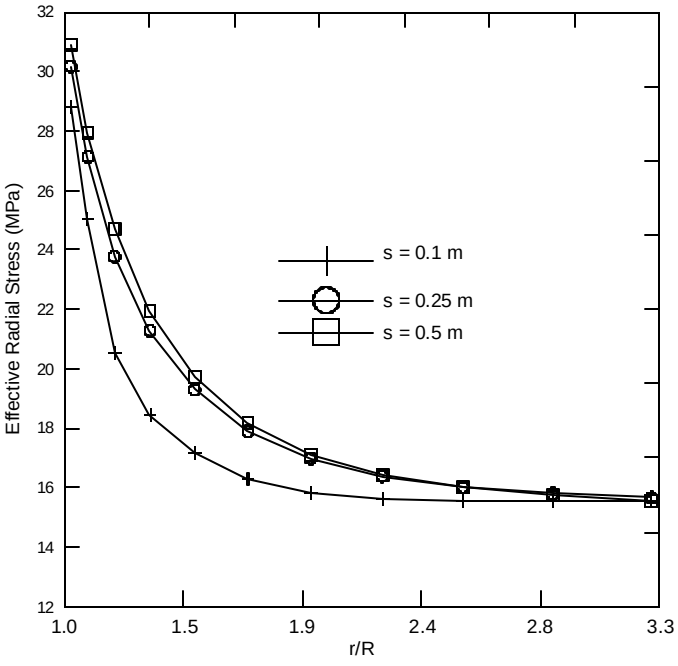

Fig. 7-Effective tangential stress distribution for different fracture spacings and initial oil saturation S_{oi} = 0.5 (dual-porosity, two-phase; s – fracture spacing).

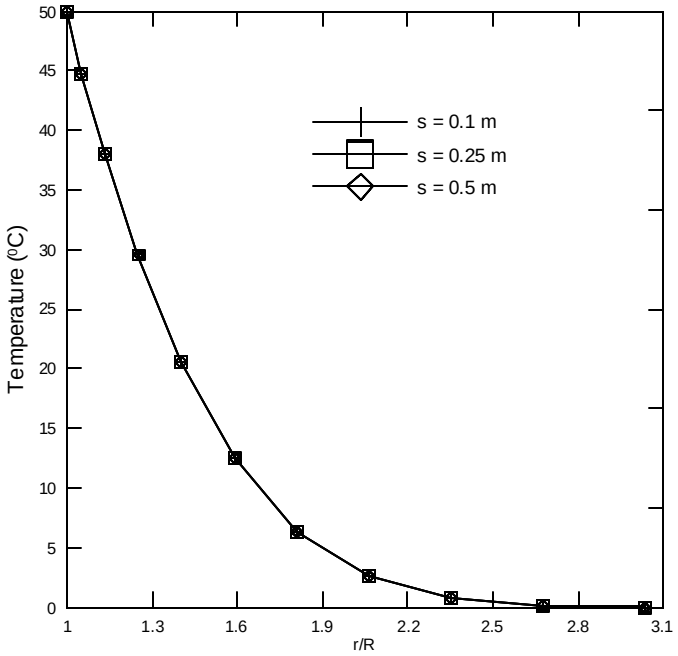

Fig. 8-Temperature distribution for different fracture spacings and initial oil saturation S_{oi} = 0.5 (dual-porosity, two-phase; s – fracture spacing).

Appendix

$$\mathrm{K} = \int_{\mathrm{v}} \mathrm{B}^{\mathrm{T}} \mathrm{D}^{\mathrm{I,II}} \mathrm{B} \mathrm{dV}$$

$$\Omega_c^{(h)} = -\int_{\mathrm{v}} \mathrm{B}^{\mathrm{T}} \mathrm{D}^{\mathrm{I,II}} \mathrm{C}^{(h)} a^{(h)} \left(S_{\Pi}^{(h)} + P_c^{(h)} \frac{\partial S_{\Pi}^{(h)}}{\partial P_c^{(h)}} \right) \mathrm{mNdV}$$

$$\mathrm{L}_{\mathrm{t}} = -\int_{\mathrm{v}} \mathrm{B}^{\mathrm{T}} \mathrm{D}^{\mathrm{I,II}} \frac{b}{3} \mathrm{mNdV}$$

$$\mathrm{K}_{\Pi}^{(h)} = \int_{\mathrm{v}} \mathrm{N}^{\mathrm{T}} a^{(h)} \left(\frac{S_{\Pi}^{(h)}}{B_{\Pi}^{(h)}} + \frac{R_q^{(h)} S_{\overline{\Pi}}^{(h)}}{B_{\overline{\Pi}}^{(h)}} \right) r_{\Pi s}^{(h)} \mathrm{m}^{\mathrm{T}} \mathrm{C}^{(h)} \mathrm{D}^{\mathrm{I,II}} \mathrm{B} \mathrm{dV}$$

$$\Omega_{\mathrm{D}}^{(h)} = \int_{\mathrm{v}} (\nabla \mathrm{N})^{\mathrm{T}} \frac{r_{\Pi s}^{(h)}}{B_{\Pi}^{(h)}} \frac{k^{(h)} k_{r\Pi}^{(h)}}{m_{\Pi}^{(h)}} (\nabla \mathrm{N}) \mathrm{dV}$$

$$\Omega_{\mathrm{eD}} = \int_{\mathrm{v}} (-1)^{(h)} \mathrm{N}^{\mathrm{T}} \frac{r_{\Pi s}^{\mathrm{I}}}{B_{\Pi}^{\mathrm{I}}} \frac{k^{\mathrm{I}} k_{r\Pi}^{\mathrm{I}}}{m_{\Pi}^{\mathrm{I}}} \Psi \mathrm{NdV}$$

$$\Omega_{tr} = \int_{\mathrm{v}} (-1)^{(h)} \mathrm{N}^{\mathrm{T}} \frac{r_{\Pi s}^{\mathrm{I}}}{B_{\Pi}^{\mathrm{I}}} \frac{k^{\mathrm{I}} k_{r\Pi}^{\mathrm{I}}}{m_{\Pi}^{\mathrm{I}}} \Psi \mathrm{NdV}$$

$$\Omega_{etr} = \int_{\mathrm{v}} (-1)^{(h)} \mathrm{N}^{\mathrm{T}} \frac{R_q^{\mathrm{I}} r_{\overline{\Pi} s}^{\mathrm{I}}}{B_{\overline{\Pi}}^{\mathrm{I}}} \frac{k^{\mathrm{I}} k_{r\overline{\Pi}}^{\mathrm{I}}}{m_{\overline{\Pi}}^{\mathrm{I}}} \Psi \mathrm{NdV}$$

$$\Omega_{\Pi}^{(h)} = \int_{v} \mathrm{N}^{\mathrm{T}} \begin{bmatrix} \left(\frac{S_{\overline{\Pi}}^{(h)} R_q^{(h)}}{B_{\overline{\Pi}}^{(h)}} + \frac{S_{\Pi}^{(h)}}{B_{\Pi}^{(h)}} \right) r_{\Pi s}^{(h)} \frac{\left(a^{(h)} - f^{(h)}\right)}{K_s^{(h)}} \\ \left(S_{\Pi}^{(h)} + P_c^{(h)} \frac{\partial S_{\Pi}^{(h)}}{\partial P_c^{(h)}} \right) - \\ f^{(h)} r_{\Pi s}^{(h)} \left(\frac{1}{B_{\Pi}^{(h)}} - \frac{R_q^{(h)}}{B_{\overline{\Pi}}^{(h)}} \right) \frac{\partial S_{\Pi}^{(h)}}{\partial P_c^{(h)}} - \\ \frac{f^{(h)} S_{\overline{\Pi}}^{(h)} r_{\Pi s}^{(h)}}{\left(B_o^{(h)}\right)^2} \frac{\partial B_{\Pi}^{(h)}}{\partial P_{\Pi}^{(h)}} + \\ \frac{f^{(h)} S_{\overline{\Pi}}^{(h)} r_{\Pi s}^{(h)}}{B_{\overline{\Pi}}^{(h)}} \frac{\partial R_q^{(h)}}{\partial P_{\Pi}^{(h)}} \end{bmatrix} \mathrm{NdV}$$

$$\overline{\mathrm{T}}_s = \int_{v} \mathrm{N}^{\mathrm{T}} \begin{bmatrix} \left(f^{I} S_g^{I} r_g^{I} + f^{II} S_g^{II} r_g^{II} \right) C_{vg} + \\ \left(f^{I} S_o^{I} r_o^{I} + f^{II} S_o^{II} r_o^{II} \right) C_{vo} + \\ + \left(1 - f^{I} - f^{II}\right) r_s C_{vs} \end{bmatrix} \mathrm{NdV}$$

$$\overline{\mathrm{C}}_{\mathrm{t}} = \int_{v} (\nabla \mathrm{N})^{\mathrm{T}} \begin{bmatrix} C_{vg} \left(r_g^{\mathrm{I}} v_g^{\mathrm{I}} + r_g^{\mathrm{II}} v_g^{\mathrm{II}} \right) + \\ C_{vo} \left(r_o^{\mathrm{I}} v_o^{\mathrm{I}} + r_o^{\mathrm{II}} v_o^{\mathrm{II}} \right) \end{bmatrix} \mathrm{NdV}$$

$$\overline{\mathrm{K}}_{\mathrm{t}} = \int_{v} \mathrm{N}^{\mathrm{T}} \left(1 - f^{I} - f^{II}\right) \beta K b T \mathrm{m}^{\mathrm{T}} \mathrm{BdV}$$

$$\overline{\mathrm{H}}_{\mathrm{tF}} = \int_{v} (\nabla \mathrm{N})^{\mathrm{T}} \begin{bmatrix} \left(f^{\mathrm{I}} S_g^{\mathrm{I}} + f^{\mathrm{II}} S_g^{\mathrm{I}} \right) l_g + \\ \left(f^{\mathrm{I}} S_o^{\mathrm{I}} + f^{\mathrm{II}} S_o^{\mathrm{I}} \right) l_o \\ + \left(1 - f^{\mathrm{I}} - f^{\mathrm{II}}\right) l_s \end{bmatrix} (\nabla \mathrm{N}) \mathrm{dV}$$

$$S_{\Pi t}^{(h)} = \int_{v} \mathrm{N}^{\mathrm{T}} \begin{bmatrix} \left(\frac{S_{\overline{\Pi}}^{(h)} R_q^{(h)}}{B_{\overline{\Pi}}^{(h)}} + \frac{S_{\Pi}^{(h)}}{B_{\Pi}^{(h)}} \right) r_{\Pi s}^{(h)} \\ \left[\begin{array}{l} \left(1 - a^{(h)}\right) b^{(h)} - \\ \left(1 - f^{(h)}\right) b_s^{(h)} \\ - \frac{\left(a^{(h)} - f^{(h)}\right)}{K_s^{(h)}} \\ P_c^{(h)} \frac{\partial S_{\Pi}^{(h)}}{\partial T} \end{array} \right] \\ - \frac{f^{(h)} r_{\Pi s}^{(h)} S_{\Pi}^{(h)}}{\left(B_{\Pi}^{(h)}\right)^2} \frac{\partial B_{\Pi}^{(h)}}{\partial T} - \\ \frac{f^{(h)} r_{\Pi s}^{(h)} S_{\overline{\Pi}}^{(h)} R_q^{(h)}}{\left(B_{\Pi}^{(h)}\right)^2} \frac{\partial B_{\overline{\Pi}}^{(h)}}{\partial T} \\ + \frac{f^{(h)} r_{\Pi s}^{(h)} S_{\overline{\Pi}}^{(h)}}{B_{\overline{\Pi}}^{(h)}} \frac{\partial R_q^{(h)}}{\partial T} + \\ f^{(h)} r_{\Pi s}^{(h)} \left(\frac{1}{B_{\Pi}^{(h)}} - \frac{R_q^{(h)}}{B_{\overline{\Pi}}^{(h)}} \right) \frac{\partial S_{\Pi}^{(h)}}{\partial T} \end{bmatrix} \mathrm{NdV}$$

where,

Ω = O, G when π = o, g respectively; m^{T} = [1 1 1 0 0 0]